Reactivity of trinuclear ruthenium acetates with nitrite and nitric oxide ligands in aqueous media

Hugo E. Barbosa,[a] Amanda B. da Silva,[a] Pedro H. O. Nazar,[a] Renan R. Bertoloni,[a]

Antonio G. S. de Oliveira-Filho[a,b] and Sofia Nikolaou[a*]

[1]*Departmento de Química, LABiQSC2 – Laboratório de Atividade Biológica e Química Supramolecular de Compostos de Coordenação, Faculdade de Filosofia, Ciências e Letras de Ribeirão Preto, Universi-dade de São Paulo, ZIPCODE 14040-901, Ribeirão Preto-SP, Brazil*

[2]*Instituto de Química de São Carlos, Universidade de São Paulo, Av. Trabalhador São-Carlense, 400, 13566-590, São Carlos, SP, Brazil.*

*sofia@ffclrp.usp.br

Support Information

Figure S1. ^{1}H NMR spectrum of a 1×10^{-2} mol.L^{-1} solution of the compound $[Ru_3O(CH_3COO)_6(py)_2NO_2]$ in $CDCl_3$, 400 MHz, 298K.

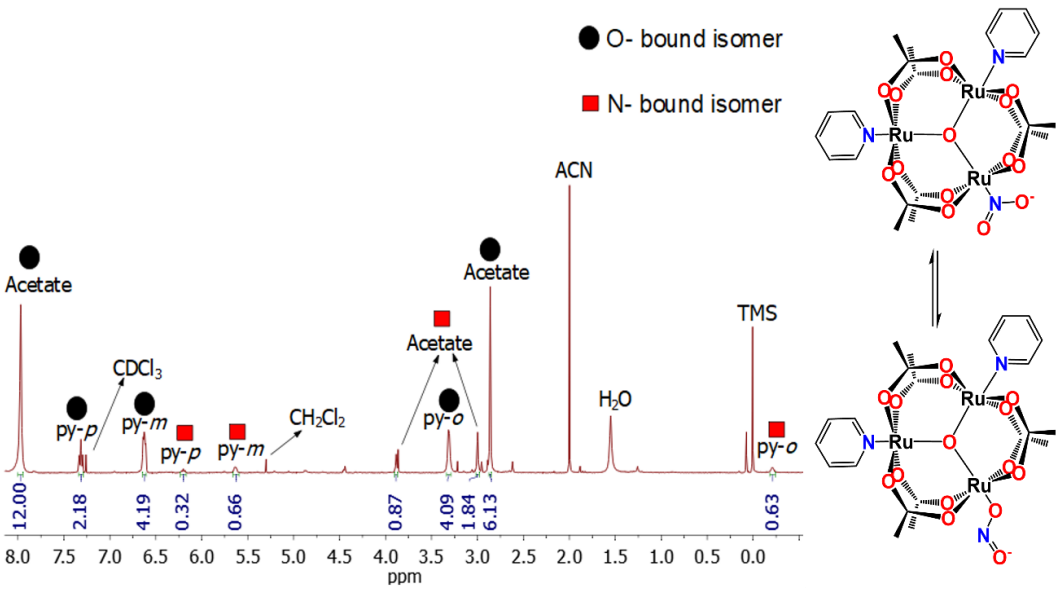

Figure S2. Schematic representation of induced magnetic field generated by electron circulation in the nitrite-N linkage isomer of compound $[Ru_3O(CH_3COO)_6(py)_2NO_2]$.

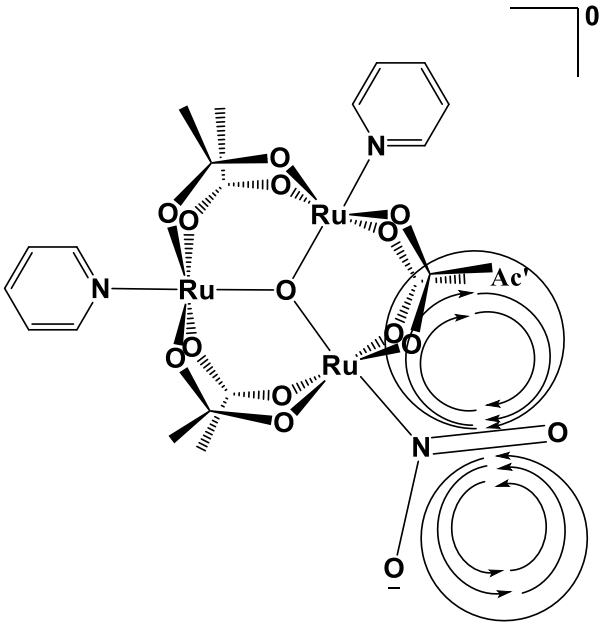

Figure S3. Interconversion equilibrium of the linkage isomers of the complex $[Ru_3O(CH_3COO)_6(py)_2NO_2]$.

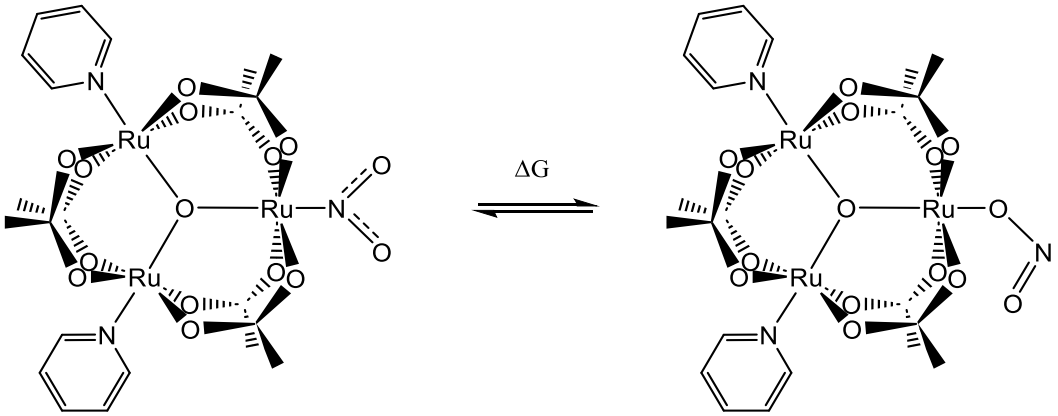

Figure S4. Comparison between the absorption spectra of the compound $[Ru_3O(CH_3COO)_6(py)_2CH_3OH]PF_6$ and the spectra obtained during the acid-base reactivity experiment of the complex $[Ru_3O(CH_3COO)_6(py)_2NO_2]$ (4.45×10^{-5} mol.L^{-1}) with the complex in ACN using HCl solution as the acid.

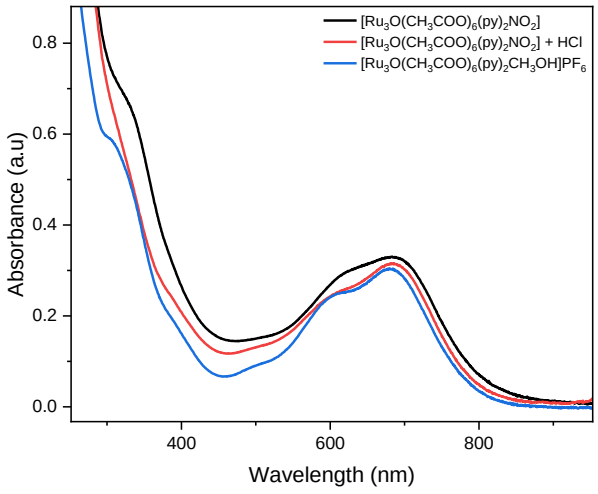

Figure S5. Schematic representation of the chemical reactions involved in the Griess test.

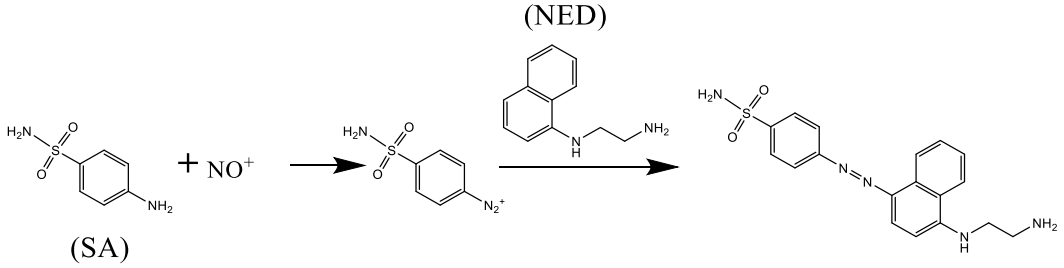

Figure S6. Photograph showing the color change during the experiment using Griess reagent for complex $[Ru_3O(CH_3COO)_6(py)_2NO_2]$ **(1)**. From left to right solutions of: Reagent, Complex **1**, Complex **1** + reagent, and positive control ($NaNO_2$).

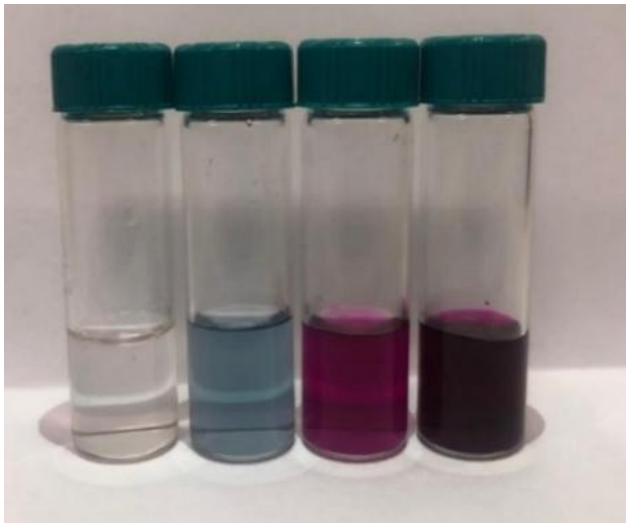

Figure S7. Electronic absorption spectra of complex $[Ru_3O(CH_3COO)_6(py)_2NO_2]$ in aqueous solution with 2% DMSO before and after addition of Griess reagent.

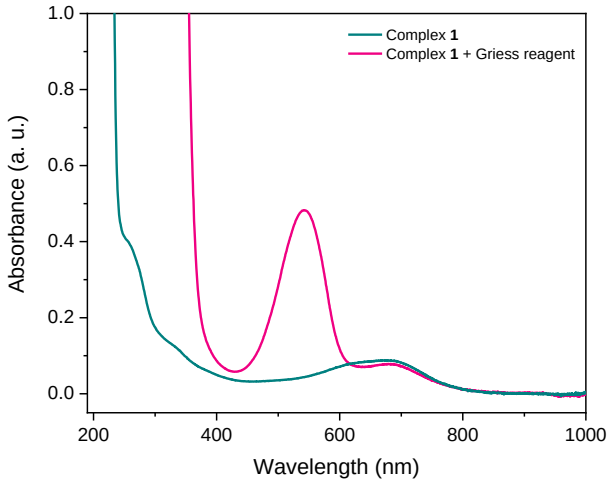

Figure S8. Comparison of the electronic absorption spectra of the compound $[Ru^{III}Ru^{III}Ru^{III}O(CH_3COO)_6(py)_2(NO_2^-]$ with $[Ru^{III}Ru^{III}Ru^{III}O(CH_3COO)_6(py)_2(NO_2^-)]^-$ reduced with hydrazine in DMSO.

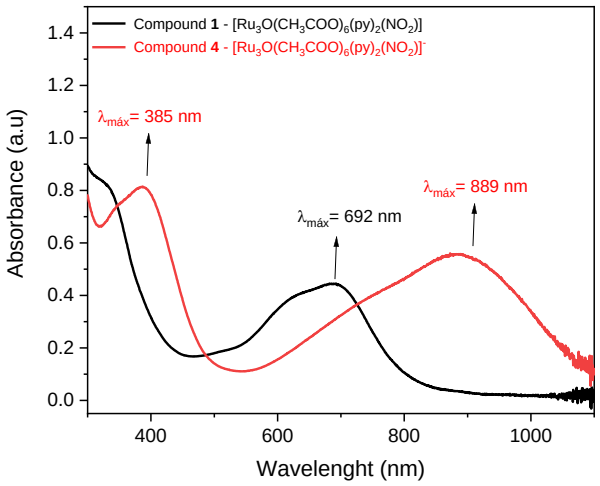

Figure S9. Electronic absorption spectra of complex $[Ru_3O(CH_3COO)_6(py)_2NO]PF_6$ **2** in tris.HCl buffer solution at pH 7.4 and 8.5 after 30 minutes and after production of **3.**

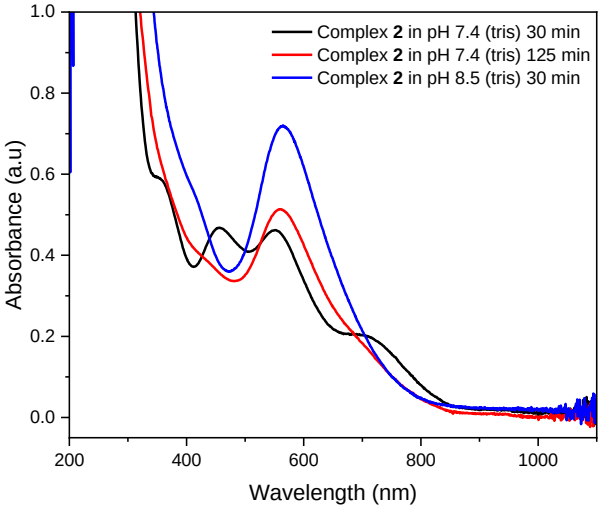

Figure S10. Electronic absorption spectra of the $[Ru_3O(CH_3COO)_6(py)_2NO]PF_6$ **2** complex in PBS buffer solution at pH 7.4 after 30 minutes and after the production of **3** (125 s).

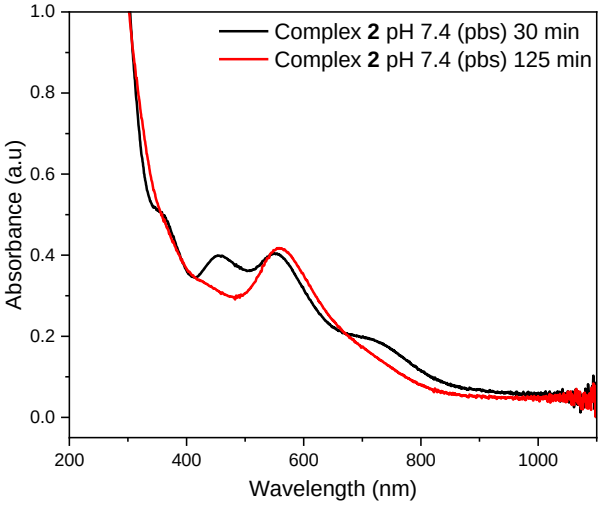

Figure S11. Kinetic curve obtained from the reactivity of the $[Ru_3O(CH_3COO)_6(py)_2NO]PF_6$ **2** complex in tris.HCl buffer solution pH 7.4 with its respective induction time of 1560 s.

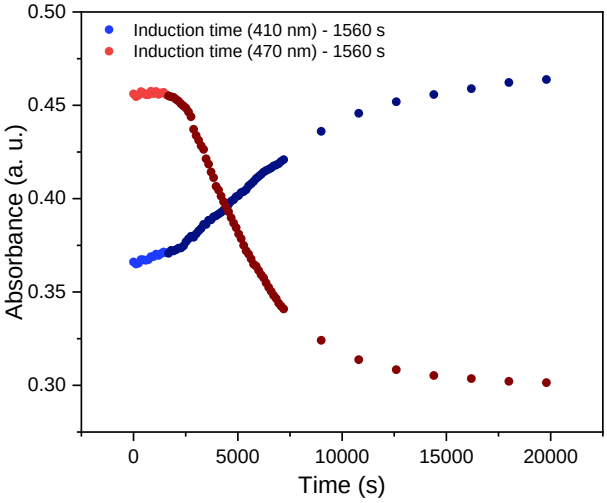

Figure S12. Kinetic curve obtained from the reactivity of the $[Ru_3O(CH_3COO)_6(py)_2NO]PF_6$ **2** complex in tris.HCl buffer solution pH 8.5 with its respective induction time of 600 s.